scattering. The electric field in the crystallites is

$$\mathcal{E}_c = \Delta V_c / l_c = j/\sigma_c. \quad \text{(A-6)}$$

Substituting Eqs. (6), (9), and (A-5) in Eq. (A-6) we obtain

$$\mathcal{E}_c = \mathcal{E}\sigma/\sigma_c = \mathcal{E}\mu^*/\mu_c. \quad \text{(A-7)}$$

$\mathcal{E}_c$ will normally be less than $\mathcal{E}$ because μ^* is less than μ_c, as shown by comparing the Hall mobility of films[10] with that of single crystals.[11] At room temperature in PbS, $\mu^* \cong 5$ while $\mu_c \cong 400$ cm²/volt-sec.

From the above and the results of Sec. II we see that a precise characterization of a film involves three conductivities, mobilities, and electric fields. The macroscopic definitions are most useful for this paper, but when microscopic properties are discussed care must be taken to insure that the correct electric field is used.

It is also possible that the current density in the barriers is greater than in the crystallites, as when the effective cross-sectional area of a barrier, A_b, is small compared to that of the adjacent crystallites. We do not attempt to discuss this effect quantitatively here.

ACKNOWLEDGMENTS

The author wishes to acknowledge the many helpful discussions he has had with Dr. J. N. Humphrey, Dr. W. W. Scanlon, Dr. J. F. Woods, and Miss Frances L. Lummis.

PHYSICAL REVIEW VOLUME 104, NUMBER 6 DECEMBER 15, 1956

Effect of Monolayer Adsorption on the Ejection of Electrons from Metals by Ions

HOMER D. HAGSTRUM
Bell Telephone Laboratories, Murray Hill, New Jersey

(Received August 23, 1956)

Electron ejection from metals by ions is shown in this work to be a surface-sensitive phenomenon which is profoundly affected by the adsorption of a monolayer of foreign gas on an atomically clean metal surface. Monolayer adsorption is shown to decrease the total electron yield, γ_i, primarily at the expense of the faster electrons ejected from the metal. Measurements of γ_i show it to decrease steadily as the monolayer forms and to level off at a value characteristic of the covered surface when the monolayer is completed. Measurements have been made for the adsorption of N_2, H_2, and CO on tungsten. Electron ejection by all the singly-charged ions of the noble gases has been studied. It was possible to clean the tungsten surface in the presence of N_2 and CO but not in H_2. In H_2 the tungsten surface, as judged from γ_i measurement, was found to be covered with about 75% of a monolayer immediately upon cooling from 2000°K. It is shown that the effect of monolayer adsorption cannot possibly be simply the result of change in work function. There is also evidence that electrons are ejected in non-Auger processes at higher ion energies when the surface is covered.

I. INTRODUCTION

As might be expected, the ejection of electrons from metals by slowly moving positive ions is a surface-sensitive phenomenon. For this reason one would like to study it not only with atomically clean surfaces[1,2] but also with surfaces having known amounts of known gases adsorbed upon them.

If foreign atoms adsorbed on a metal surface change the work function, the probability of escape of electrons excited inside the metal is also changed. For secondary emission by a beam of primary electrons this is the only effect of surface coverage since the surface film has negligible effect upon the production of internal secondary electrons in the body of the metal.[3] It seems clear that one is not justified in drawing any such conclusion *a priori* for the Auger ejection of electrons by slowly moving positive ions. Here the primary process of excitation of the internal secondary electron takes place with the ion just *outside* the metal surface and proceeds with a probability which depends upon whether the excited electron may escape from the metal or not.[4] Thus it is certainly possible that the interposition of a layer of foreign atoms between the metal lattice and the incoming ion will affect not only the probability of electron escape but also other aspects of the phenomenon (Sec. VII). It is also possible that non-Auger processes of electron ejection become important for the gas-covered surface.

The results reported in this paper concern the effect of adsorption of the common gases H_2, N_2, and CO on the electron ejection from tungsten by singly-charged ions of the noble gases. Experimental apparatus is discussed in Sec. II and experimental conditions prevailing when measurements were made are discussed in Sec. III. It is shown that experimental conditions can be established in which it is possible to produce a monolayer of adsorbed gas of a high degree of purity. The effects of the presence of this monolayer on the total yield of electrons for incident ion (Sec. IV) and on

[1] H. D. Hagstrum, Phys. Rev. **96**, 325 (1954); **104**, 317 (1956).
[2] H. D. Hagstrum, Phys. Rev. **104**, 672 (1956).
[3] On this basis P. A. Wolff, Phys. Rev. **95**, 56 (1954), has successfully accounted for the observed rate of change of secondary electron yield with work function.
[4] H. D. Hagstrum, Phys. Rev. **96**, 336 (1954).

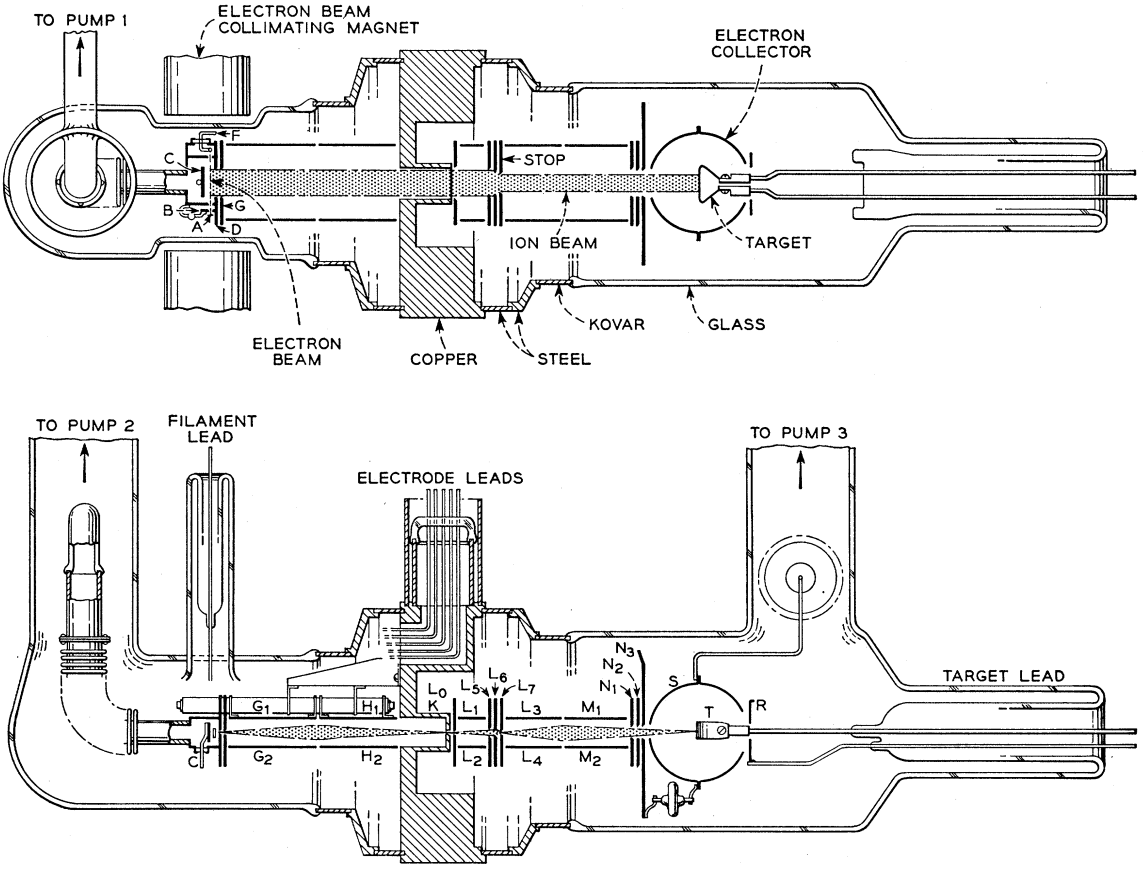

FIG. 1. Schematic diagram of one of the pieces of apparatus used in this work. It is the so-called Instrument V used for the later work with N_2. It differs from the other apparatus used (Instrument III) in that the ion source and target are in different chambers and constructional features have been improved. Compare Fig. 4 of reference 5. Critical apertures in this apparatus are the same as those of Instrument II specified in Table II of reference 5. The slit in electrode K separating source and target chambers is 0.12×10 mm. A photograph of this apparatus appeared on the cover of the February, 1955 issue of the Journal of Applied Physics.

the energy distribution of the ejected electrons (Sec. V) have been studied. The work is most extensive for the case of N_2 on tungsten in which the effect is studied for all the singly-charged noble gas ions and as a function of ion kinetic energy. For H_2 and CO the work was limited to the ions He^+ and Ne^+ of 200-ev kinetic energy.

As judged by the electron ejection results a tungsten surface is atomically clean after heating above 2000°K and cooling to room temperature in the presence of N_2 and CO but not in the presence of H_2. The evidences of this anomalous behavior of tungsten in H_2 and a possible reason for it are discussed in Sec. VI. It does not seem possible now to give a detailed theoretical account of the effect of monlayer adsorption on Auger ejection. The discussion in this paper is limited to an account of the effect of work function change based on the theory for clean metals already published,[4] and to a suggestion as to a further and perhaps more significant effect of monolayer adsorption upon the production of the internal secondary electrons (Sec. VII). Notation used in this paper is defined as introduced.

II. EXPERIMENT AND APPARATUS

The experimental work reported in this paper was carried out with two pieces of apparatus. The first is that already described as Instrument III in a published paper[5] on instrumentation and experimental procedure (see Fig. 4 of reference 5). With this apparatus work was done for N_2, H_2, and CO using He^+ and Ne^+ ions of 200-ev energy. The second apparatus, which we shall call Instrument V, is much like the first but incorporates a number of improvements to be discussed presently. It is shown schematically in Fig. 1. Metal parts of Instrument III were made of tantalum, those of Instrument V of nichrome V.

In both Instruments III and V, ions formed in a magnetically collimated electron beam are focused upon a target by two electrostatic lenses in tandem. In neither instrument is the ion beam magnetically analyzed with respect to the ratio of mass to charge (m/e). In Fig. 1 filament A supplies electrons for the ionizing beam which passes through slits in electrodes

[5] H. D. Hagstrum, Rev. Sci. Instr. 24, 1122 (1953).

B and C to the collector F. Ions formed in the electron beam inside the chamber C are drawn out and focused by the G-H lens upon the narrow slit in K. The L-M lens serves to focus the ion beam upon the front surface of the ribbon target T which may be heated by passing current through it. Electrons ejected from T are collected by the collector S. The ions are accelerated in the G-H lens but may be accelerated or decelerated in the L-M lens depending upon the final ion energy desired at the target surface. The use of two ion lenses in tandem has the advantages of permitting variation of the ion energy at the target surface (in the L-M lens) without disturbing conditions in the ion source and of separating the source and target by a distance sufficient to reduce to negligible proportions the strength at the target of field fringing from the electron beam collimating magnet.

In both Instruments III and V the noble gas is admitted through the cold trap in the lead to pump 1 (Fig. 1) into an enclosed ionization chamber. When gas is being admitted pump 1 is usually cut off by a mercury cutoff. Instrument V differs from Instrument III in that differential pumping is provided between the source and target chambers. These communicate in Instrument V through the slit in electrode K. This noticeably reduces the effect at the target of adsorbable impurities admitted with the noble gas. The adsorbable gases, N_2, H_2, or CO are admitted through a cold trap in the lead to pump 3 directly into the target chamber.

The L-M lens of Instrument V (Fig. 1) is essentially that of Instrument II described in the instrumentation paper.[5] It differs somewhat from that of Instrument III (compare Fig. 1 of this paper with Fig. 4 of reference 5).

Several constructional improvements over Instrument III were incorporated in Instrument V. All electrodes requiring careful alignment are mounted on quartz rods which are mounted, in turn, from the central copper detail (electrode K). Thus all alignment checks can be made conveniently before the glass envelope is attached. The glass envelope is used as a structural element as little as possible. The only concessions made in this regard are the mounting of the electron beam filament and target on glass stems. This permits removal for repair or replacement without disturbing the main tube or glass envelope. Some of the constructional details of Instrument V are suggested in Fig. 1.

Since the ion beam is not magnetically analyzed, a homogeneous beam of singly-charged ions is attained by keeping the energy of the bombarding electron beam below the second ionization energy of the parent gas. However, to assure that metastably excited ions are not produced in A, Kr, or Xe one must operate with the electron energy below the excitation energy of the metastable states.[6] The electron beam energies used in these experiments are the following: He, 100 ev; Ne, 100 ev; A, 32 ev; Kr, 28 ev; and Xe, 22 ev. The noble gases admitted to the ionization chamber were of such high purity and the background gas pressure in the apparatus was so low that no detectable contamination of the beam by ions from other gases was possible.

Liquid nitrogen was used on the traps for He and Ne, CO_2, and acetone for A, Kr, and Xe. Gases used were those commercially available as spectroscopically pure supplied in liter flasks except for CO which was obtained in a so-called "lecture" tank. The gases were transferred under good vacuum conditions ($<10^{-8}$ mm Hg) through cold traps into flasks at about 300 mm Hg pressure for convenient use with the porcelain leak gas inlet system.[5,7] Mass spectrometer analyses of the gases used are given in Table I.

Electron yield, γ_i, and energy distributions functions, $N_0(E_k)$, have been determined in this work by methods discussed in the earlier publications. See, for example, references 1 and 5. γ_i for ions of a given energy has been measured as a monolayer of a known gas forms. It has also been measured as a function of ion energy with a monolayer present on the target for comparison with similar measurements on the atomically clean target. $N_0(E_k)$ functions have been measured with monolayers of the various gases on the target and compared with results for the atomically clean surface.

III. EXPERIMENTAL CONDITIONS

It is clear that one must attain a sufficiently low pressure of residual gases in the apparatus if a monolayer of high purity of a known gas is to be adsorbed in a time long enough to permit measurements while it is forming. In this work the final test of the vacuum has

TABLE I. Mass spectrometer analyses of gases used.[a]

Sample	% present								
	He	Ne	N_2	H_2	CO	O_2	CO_2	H_2O	CH_4
He	100	...	...	...	...	...	...	...	...
Ne	1.3	98.7	0.001	...	...	0.0008	<0.0006	0.002	...
N_2	...	...	99.9	...	...	...	...	...	...
H_2	...	...	...	99.7	...	...	...	0.21	...
CO	...	...	0.52	3.19	96.0	...	0.24	...	...
Minimum % detectable	0.003	0.002	0.0006	0.001	0.0006	0.0007	0.0006	...	0.0007

[a] Made with a Consolidated Engineering Corporation Instrument, Model 21-103.

[6] H. D. Hagstrum, Phys. Rev. **104**, 309 (1956).
[7] H. D. Hagstrum and H. W. Weinhart, Rev. Sci. Instr. **21**, 394 (1950).

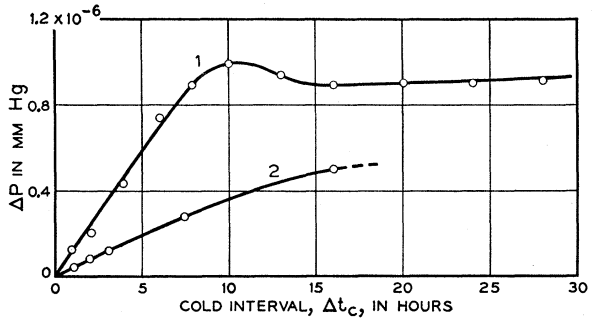

FIG. 2. Adsorption rate measurements for residual gases in the apparatus. Plotted here is pressure rise on flash as a function of cold interval before flash. Curve 1 is typical of that which obtained during the course of the experiment. Curve 2 is one obtained after rigorous processing before any adsorbable gas was admitted to the instrument.

been the measured rate of adsorption of gas on the target surface as evidenced by Δp *vs* Δt_c curves such as those of Fig. 2. The nature of these measurements and the vacuum processing employed have been discussed elsewhere.[5] In Fig. 2, curve 1 indicates a monolayer adsorption time for residual gases of about 8 hours with liquid N_2 on the traps. Residual pressure readings on the Bayard-Alpert gauge were of the order of 2×10^{-10} mm Hg. Curve 2 was taken after another baking of the apparatus and further heating of filaments and target but before any adsorbable gas was again admitted to the system. It indicates a considerably reduced adsorption rate and the suggestion of a reduced Δp value at saturation. However, during the course of the experiment, when adsorbable gases were being admitted and pumped out almost daily, the condition represented by curve 1 of Fig. 2 represents the best condition which could be maintained. The data plotted in Fig. 2 were taken with Instrument III but very similar conditions prevailed during the work with Instrument V.

In this work the tungsten target was cleaned by heating. In the preliminary stages of the experiment the target was heated for several days at about 1700°K and for a total time of nearly one hour at temperatures above 2000°K. During the course of the experimentation it was continually flashed to 2000°K in the experiment with Instrument III, to 2300°K with Instrument V. Evidence referred to elsewhere[1] indicates that this treatment removes oxygen and thus presumably any other of the common adsorbable gases. The work function determined from a Richardson plot agrees well with that accepted for clean tungsten.

Another important element in specifying the experimental conditions is the determination of the amounts of adsorbable impurities present in the apparatus or admitted with the gases used in the experiment. This is accomplished by making measurements of adsorption rate on the target under various conditions. Data taken with liquid N_2 on the traps for Instrument III are plotted in Fig. 3, for Instrument V in Fig. 4. Here the curve labelled "background" was taken with no gases being admitted but with the source filament heated. These curves indicate an initial adsorption rate comparable with that of curve 1 of Fig. 2. Thus very little adsorbable gas is being desorbed from the source filament or surrounding parts.

Also shown in Figs. 3 and 4 are the adsorption rate measurements made with helium and neon admitted to the ionization chamber. These are the curves labelled He and Ne. Pressures in the target chamber are recorded in Table II. It is apparent that the helium contains a very small admixture of adsorbable impurity gases. The curve for neon admission indicates either the admission of a larger amount of adsorbable impurity with the neon than was admitted with the helium or the adsorption at low sticking probability of the neon itself. The latter is considered relatively improbable in view of the small polarizability of Ne and the consequent small Van der Waal's attraction to a clean metal surface. There is some evidence in the mass spectrometric analyses of Table I of a greater amount of adsorbable impurity present in the Ne than in the He. There is also evidence in Figs. 3 and 4 that the differential pumping of Instrument V reduces the effect at the target of impurities admitted to the ionization chamber.

When A, Kr, and Xe are used, it is necessary to cool the traps with CO_2 and acetone. This admits Hg vapor to the instrument and reduces the monolayer adsorption time

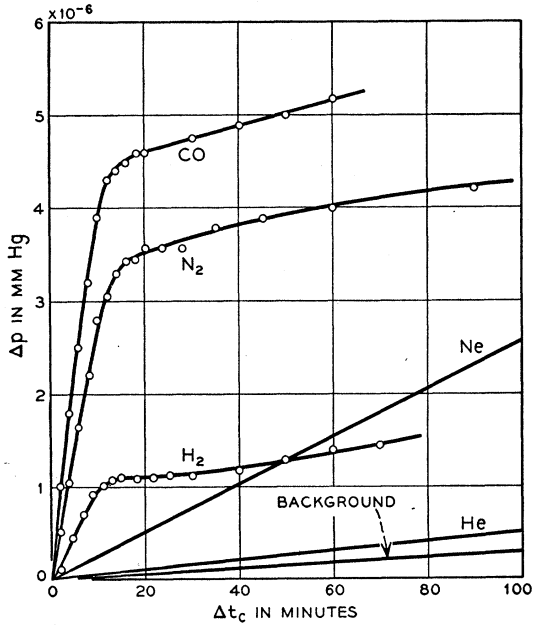

FIG. 3. Adsorption rate measurements (pressure rise on flash *vs* cold interval) made with Instrument III (liquid N_2 on traps). Curves labelled N_2, H_2, and CO were taken with these adsorbable gases being admitted to the target chamber. Pressures of CO, N_2, and H_2 were those specified in Table II giving monolayer adsorption times of about 10 minutes. The curve labelled "background" was taken with no gases admitted and with source filament hot. Curves marked He and Ne were taken with the noble gas only admitted.

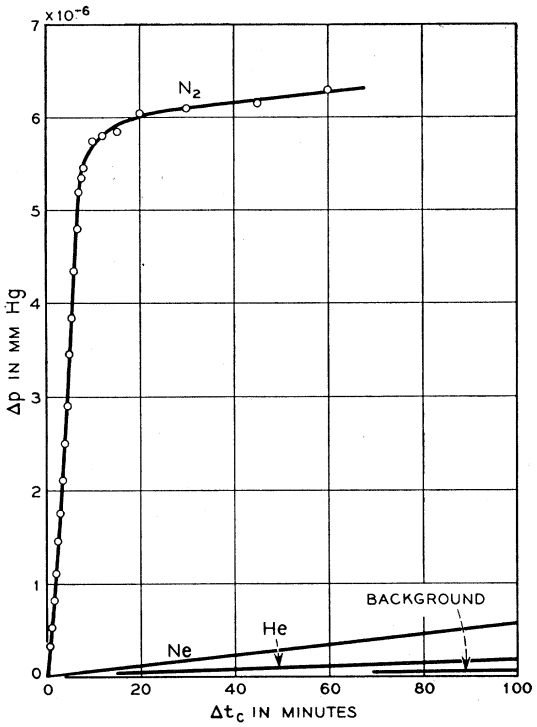

FIG. 4. Adsorption rate measurements for Instrument V with liquid N_2 on the traps. Curves have same meaning as those in Fig. 3.

measured for the residual gases as has already been reported.[1] Measurement of γ_i with and without admission of the adsorbable gas as shown in Fig. 9 enables one to judge the effect of impurities present in the apparatus or admitted with the noble gas. This is discussed below in connection with monolayer purity.

The curves labeled H_2, N_2, and CO in Fig. 3 and N_2 in Fig. 4 indicate the adsorption rates on the target for these gases when they only are admitted to the target chamber and no noble gas is admitted to the ionization chamber. The pressure was adjusted so that a convenient monolayer adsorption time of the order of 10 minutes was achieved. The time required for the Δp *vs* Δt_c curve to reach the point at which it begins to depart from its initially almost linear rise is taken to define the monolayer adsorption time. It is the time required for the surface to cover to the point where its sticking probability (proportional to the slope of the $\Delta p - \Delta t_c$ curve) reduces from a high to a relatively low value). Gas pressures in the target chambers under various conditions are listed in Table II. Note that the pressure varies by a factor of about two between conditions of target pumping and target covered when an adsorbable gas is admitted to the system but that no such pressure change with time is observed when a nonadsorbable (noble) gas is admitted. Pressures for the "target pumping" are read immediately after a flash when the target is adsorbing gas from its surroundings. Pressures for "target covered" are read after a monolayer has formed, that is, after one has reached the flatter portion of the Δp *vs* Δt_c curve at $\Delta t_c > 20$ min (see Fig. 3).

We see in Fig. 3 that about the same number of N_2 and CO molecules are released when a monolayer is flashed off the tungsten target. Considerably less gas is measured in the ionization manometer for H_2. This does not necessarily mean that there are fewer molecules per monolayer for H_2 than for the other gases. The effect is most likely due either to absorption of a fraction of the monolayer into the body of the tungsten or to the dissociation of a fraction of the H_2 to atomic hydrogen as the target is flashed or both. (Sec. VI.) The pressure rise on flash is a function of several parameters including pumping speed of the pumps and the rate of temperature rise of the target. Some of the variation of Δp for flash-off of a monolayer to be seen in Figs. 3 and 4 is most likely the result of variation of pumping speed depending upon the amount of mercury condensed in the liquid air traps.

When the effect of monolayer adsorption is being studied the source filament is heated, a noble gas is admitted to the source chamber, and an adsorbable gas (N_2, H_2, or CO) is admitted into the target chamber. The monolayer which then forms on the target surface will consist of the desired adsorbable gas as well as such adsorbable impurity gases as are admitted with either the noble gas or the desired adsorbable gas, or are present in the residual gases or released from the electrodes heated by the source filament. We should like to assess the purity of the monolayer, i.e., to determine what fraction of it consists of the desired adsorbable gas admitted to the target chamber. The data of Figs. 3 and 4 enable one to determine what fraction of the final monolayer is adsorbed from gases admitted with the noble gas or present for other reasons in the instrument. One cannot determine, however, the amount of impurity gas admitted with the desired

TABLE II. Gas pressures (mm Hg) in the target chamber.[a]

	Instrument III		Instrument V	
	Target pumping[b]	Target covered[c]	Target pumping[b]	Target covered[c]
Residual gases (liquid N_2 on traps)	$2-6\times10^{-10}$	$2-6\times10^{-10}$	$<5\times10^{-11}$	$<5\times10^{-1}$
Residual gases (CO_2+acetone on traps)	...	...	...	$3-5\times10^{-9}$
N_2 admitted to target chamber	0.6×10^{-8}	1.2×10^{-8}	2.8×10^{-8}	7.8×10^{-8}
H_2 admitted to target chamber	0.8×10^{-8}	1.2×10^{-8}	...	...
CO admitted to target chamber	1.0×10^{-8}	2.1×10^{-8}	...	...
He admitted to ionization chamber[d]	1.1×10^{-6}	1.1×10^{-6}	6.7×10^{-8}	6.7×10^{-8}
Ne admitted to ionization chamber[d]	2.9×10^{-6}	2.9×10^{-6}	1.1×10^{-7}	1.1×10^{-7}

[a] Ionization gauge reading corrected for ionization efficiency of gas where it is known. For the residual gases the pressure specified is equivalent N_2 pressure.
[b] Data taken immediately after a target flash.
[c] Data taken when the target was covered with a monolayer of residual gas or of adsorbable gas being admitted to the target chamber.
[d] Note that these pressures in the target chamber are considerably lower for Instrument V which has differential pumping between source and target chambers than for Instrument III which does not.

adsorbable gas. Table I indicates the purity of the N_2, H_2, and CO used. In Fig. 3, for example, we see that when N_2 and He are being admitted the monolayer is very largely N_2. In the 10 minutes required for the monolayer to form the amount of impurity gas is about 3% of a monolayer. This fraction is the value to which Δp has risen on the curve labeled He divided by the Δp value at 10 min on the N_2 curve. Since the N_2 itself is very pure we conclude the N_2 monolayer is about 97% pure when He is used. A similar determination for CO, taking account of the fact that the CO is only 96% pure (Table I) indicates that the CO monolayer is

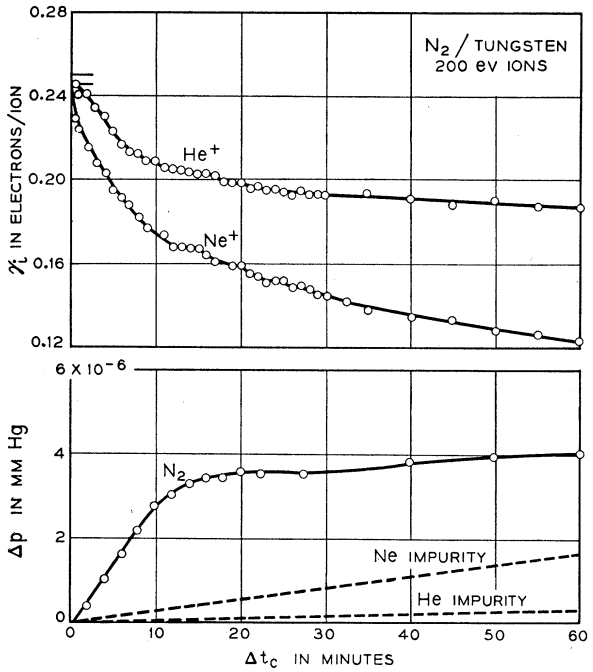

FIG. 5. Plots of γ_i for He^+ and Ne^+ ions (top) and pressure rise on target flash (bottom) as functions of cold interval as a monolayer of N_2 forms on tungsten. Data taken with Instrument III for 200-ev ions. Curves in the lower graph are those of Fig. 3. Horizontal lines on γ_i axis indicate γ_i values for clean tungsten measured when N_2 was not admitted.

about 93% pure in the presence of He. If the H_2 monolayer contains about as many molecules per monolayer as does that for Ne or CO and the low Δp on saturation in Fig. 3 has other causes (Sec. VI), we conclude that the H_2 monolayer is also about 97% pure in the presence of He.

When Ne is admitted to the ion source we must conclude that the monolayers which form on the target from N_2, H_2, or CO are less pure than for He. Here we conclude from Fig. 3 that the N_2 and H_2 monolayers are about 87% pure and the CO monolayer about 83%. Purer monolayers of N_2 with either He or Ne present and with liquid N_2 on the traps are obtained with Instrument V, as Fig. 4 indicates, because of the differential pumping between the source and target chambers. Here the monolayer appears to be better

TABLE III. Purity of monolayers formed in this experiment.

Adsorbable gas admitted	Noble gas admitted	Purity of monolayer in percent of desired adsorbable gas: Instrument III	Instrument V
N_2	He	97	>98
	Ne	87	>98
	A	...	~75
	Kr	...	~75
	Xe	...	~65
H_2[a]	He	93	...
	Ne	87	...
CO	He	93	...
	Ne	83	...

[a] These purity figures are based on the assumption that an N_2 and an H_2 monolayer contain the same number of molecules. The low value of Δp on saturation in Fig. 3 is thus assumed to be the result of other causes discussed in Sec. VI.

than 98% pure in any case. The purity of the N_2 monolayer adsorbed in the presence of A, Kr, and Xe in Instrument V and with CO_2 and acetone on the traps may be judged from Fig. 9. Here γ_i is plotted in one case as a function of time after a target flash as the target surface covers in the presence of residual gases and adsorbable gases admitted with the noble gas, and in the other case in the presence of these gases and the desired adsorbable gas admitted to the target chamber. A rough estimate of the fraction of impurities in the monolayer should be the ratio of the change in γ_i in the first case divided by that in the second case during the

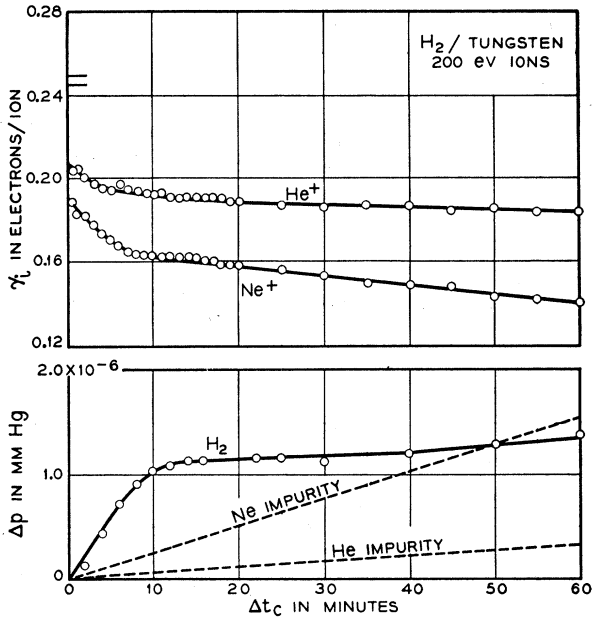

FIG. 6. Plots of γ_i for He^+ and Ne^+ ions (top) and pressure rise on target flash (bottom) as functions of cold interval as H_2 is adsorbed on tungsten. Curves of lower graph are from Fig. 3. Horizontal lines on γ_i axis indicate γ_i values for clean W obtained before H_2 experiment commenced. Note that immediately after a target flash the γ_i for clean W is not obtained in contradistinction to the behavior in N_2 and CO (Figs. 5 and 7). Data taken with Instrument III for 200-ev ions.

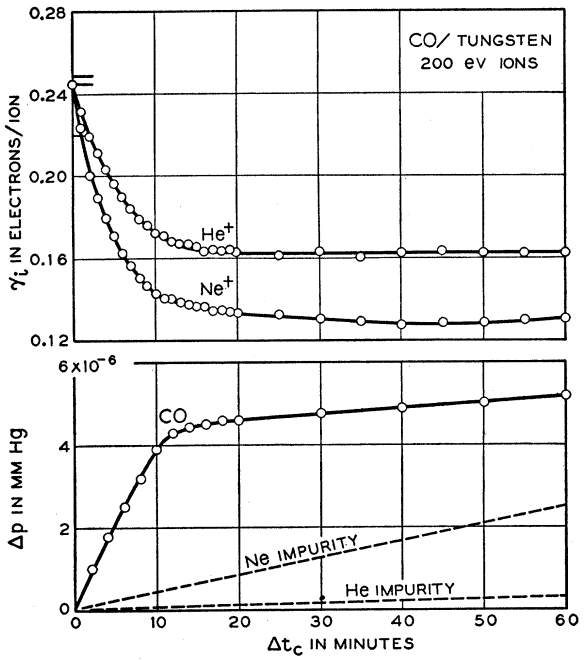

FIG. 7. Plots of γ_i for He^+ and Ne^+ ions (top) and pressure rise on target flash (bottom) as functions of cold interval as a monolayer of CO forms on tungsten. Curves of lower graph are from Fig. 3. Horizontal lines on γ_i axis give γ_i values for clean tungsten as obtained immediately after a target flash when CO was not admitted to the system. Instrument III used and energy of ions was 200 ev.

time necessary to form the monolayer. From Fig. 9 it is estimated in this way that the N_2 monolayer is about 75% pure when A and Kr are present and about 65% pure in the presence of Xe.

The estimates made above of monolayer purity are summarized in Table III.

IV. EFFECT OF MONOLAYER ADSORPTION ON TOTAL ELECTRON YIELD

Two types of measurements have been made which indicate the effect of monolayer adsorption on total electron yield, γ_i, from Auger ejection. These are: 1. The variation of γ_i with time as a monolayer forms (Figs. 5–9), and 2. The variation of γ_i with ion kinetic energy with the target clean and with it covered with a monolayer of a known gas (Figs. 10 and 11). In Figs. 5, 6, and 7 the variation of γ_i on adsorption of N_2, H_2, and CO, respectively, are shown for He^+ and Ne^+ ions of 200-ev incident energy. These data were obtained in the earlier portion of the experiment using Instrument III. Similar data for N_2, using He^+ and Ne^+ ions of 10-ev energy obtained with Instrument V, are shown in Fig. 8. In each of these graphs below the γ_i plot there is shown the variation of Δp on target flash plotted to the same time scale. These latter curves thus show the adsorption rate of gas on the target surface. The time at which the $\Delta p - \Delta t_c$ curve departs from the more or less linear initial rise gives the monolayer adsorption time.

We note in each case that the γ_i value tends to level off in about the time required for the monolayer to form. In Figs. 5 and 6 this leveling off, especially with Ne gas present, is least pronounced. This may well be due to the fact that here the monolayer is least pure. one is tempted to speculate that the monolayer once formed is slowly altered in composition with time by replacement of N_2 with another component present in the impurity gases. Since γ_i with CO present saturates well (Fig. 7) whereas N_2 does not (Fig. 5) it might appear that CO can replace N_2 adsorbed on a metal surface.

In Fig. 9 are plotted the variations of γ_i for A^+, Kr^+, and Xe^+ ions of 10-ev incident energy. Here there are plots of two runs for each ion. One was made with only residual gases, the noble gas, and any impurity gases admitted with the noble gas present in the apparatus, the second with N_2 also admitted to the target chamber. We note from the relatively rapid drop of γ_i with time in the first of these cases that either sizable amounts of

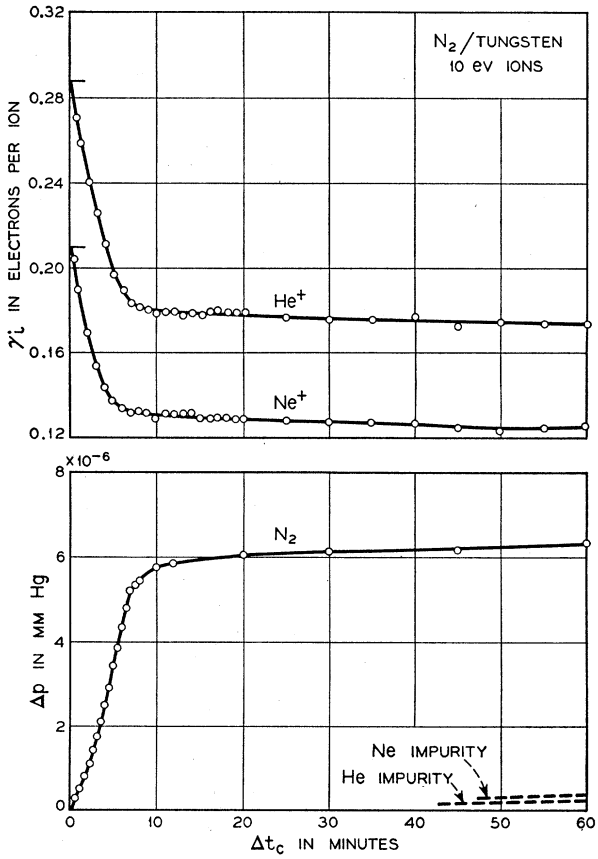

FIG. 8. Plots of γ_i for He^+ and Ne^+ ions and pressure rise on target flash as functions of cold interval as a monolayer of N_2 forms on tungsten. Data taken with Instrument V using ions of 10-ev energy. Curves of lower graph from Fig. 4. Horizontal lines on γ_i axis give γ_i values for clean W measured when N_2 was not admitted to the target chamber.

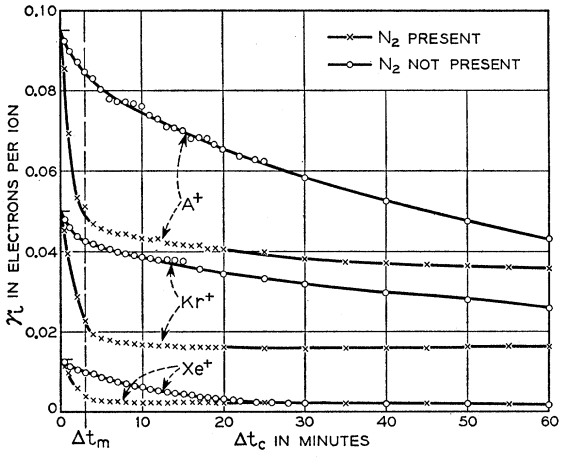

FIG. 9. Plots of variation of γ_i with cold interval for A^+, Kr^+, and Xe^+ ions of 10-ev energy measured with Instrument V. Upper curve in each case indicates change in γ_i due to adsorption from residual gases in the instrument, adsorbable gases admitted with the noble gas, or possible adsorption at low sticking probability of the noble gas itself. The lower curves, taken when N_2 was admitted, show in each case the additional effect of adsorption of the N_2.

adsorbable impurities were present or the noble gas is itself adsorbed with low sticking probability. This is particularly true in the case of xenon, the most polarizable of the noble gases. From the time taken for the γ_i curve to level off we may determine the monolayer adsorption time. These appear to be about 80 minutes for argon and krypton, 25 minutes for xenon.

The curves of Fig. 9 taken with N_2 present indicate a much more rapid drop of γ_i with time. The pressure of N_2 was increased here over that used for helium and neon with liquid N_2 on the traps in an attempt to produce purer monolayers by forming them faster. The use of data of Fig. 9 in the estimation of monolayer purity has already been discussed.

We note that in all cases the electron yield, γ_i, decreases as a monolayer forms on the target surface. In each case except with H_2 present (Fig. 6) the γ_i *vs* Δt_c curve extrapolates back to a γ_i value at $\Delta t_c=0$ which is very nearly that measured when no adsorbable gas is admitted. These latter values, indicated by the short horizontal lines on the γ_i axis, in turn agree well with those measured in the work on tungsten already published[1] (see data for clean W in Figs. 10 and 11). The anomalous behavior in the case of H_2 is discussed in Sec. VI

In Figs. 10 and 11, γ_i is plotted as a function of ion kinetic energy for the clean target and the target covered with N_2. The data with a monolayer present were measured at times after a target flash on the flat portion of the Δp *vs* Δt_c curve after the monolayer has formed. As Figs. 8 and 9 indicate, this is also the time during which γ_i is relatively constant. The data for the clean target in Figs. 10 and 11 were taken from the published work on tungsten.[1]

We see in Figs. 10 and 11 that adsorption of a monolayer reduces γ_i at all ion energies up to 1000 ev but more markedly at low ion energies for He^+, Ne^+, and A^+. We note also the change in the case of He^+ from an initially decreasing characteristic to a monotonically increasing one. The variation of γ_i for He^+ ions at low ion energies has consistently shown itself to be a very sensitive test of the cleanliness of a metal surface. The significance of the changes in γ_i dependence on ion energy caused by monolayer formation are discussed in Sec. VII.

V. EFFECT OF MONOLAYER ADSORPTION ON ELECTRON ENERGY DISTRIBUTION

Data on electron energy distribution have also been obtained with a monolayer of gas adsorbed on the tungsten surface. These are shown for N_2 plotted in Figs. 12–14. For proper comparison of the distributions for the clean and covered metal one should shift the N_2/W curves on the energy scale by an amount $-\Delta\varphi$, the negative of the increase in work function occurring on adsorption of the nitrogen monolayer. The effect of work function change should be observable in a dis-

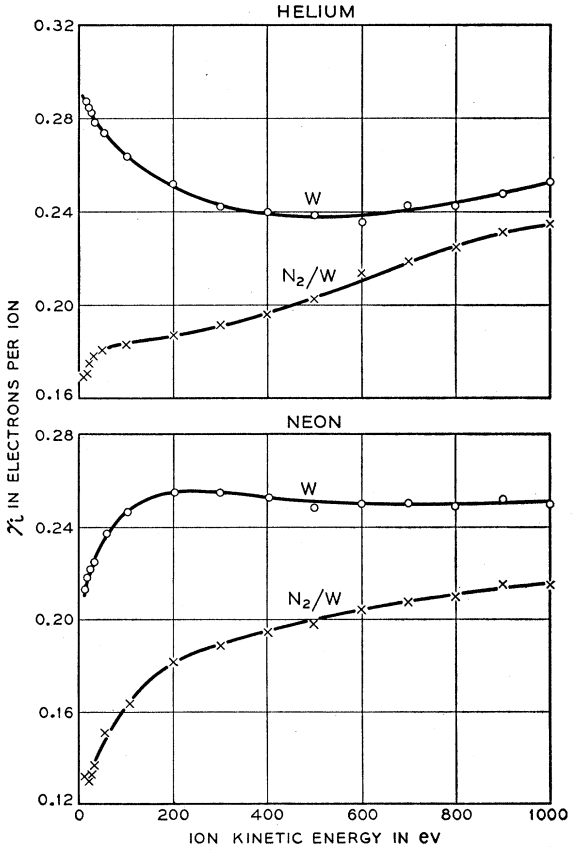

FIG. 10. Variation of γ_i with ion energy for clean tungsten (W) and tungsten covered with a monolayer of N_2 (N_2/W). Upper graph for He^+ ions, lower for Ne^+. Data for covered surface taken on flat portion of Δp *vs* Δt_c curve such as that in lower graph of Fig. 8 for $\Delta t_c>15$ min.

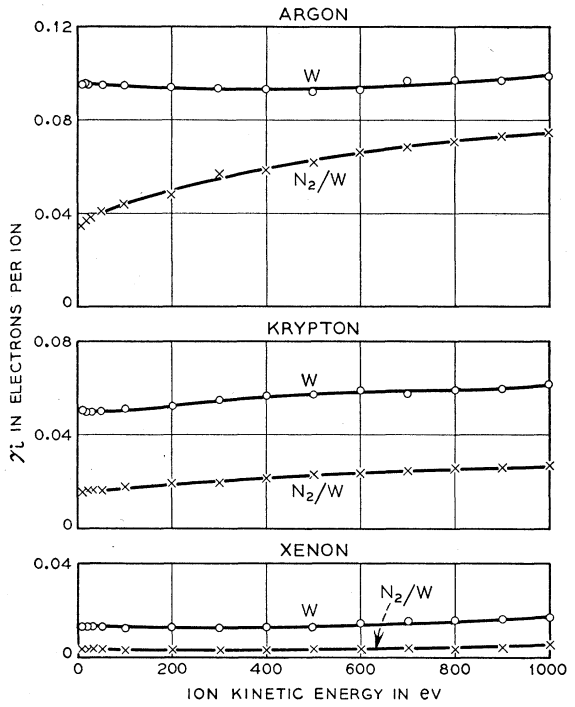

FIG. 11. Plots of γ_i for A^+, Kr^+, and Xe^+ ions as functions of ion energy for clean tungsten (W) and tungsten covered with an N_2 monolayer (N_2/W).

placement of the low-energy limits of the $N_0(E_k)$ curves *provided* the number of excited electrons inside the metal near $E_k=0$ is not greatly different for the two surface conditions. This requirement is most closely met for A^+ ions from which curves a rough estimate of a 0.4-ev increase in φ on N_2 monolayer adsorption is obtained.[8]

We see that the effect of monolayer adsorption is to change quite radically the form of the energy distribution. This change consists largely in the removal of the faster electrons from the distribution. Electrons as fast as those produced with a clean surface appear when the surface is covered but in smaller amounts. We shall see in Sec. VII that these results cannot be explained as the result of a work function change only but require more fundamental changes in the ejection mechanism for the gas-covered surface.

VI. ANOMALOUS BEHAVIOR OF TUNGSTEN IN THE PRESENCE OF HYDROGEN

We have noted in the discussion of Figs. 5–8 that in N_2 and CO it was possible to clean a tungsten surface by flashing to high temperature but that in hydrogen it was not. The basic evidence for this is that with N_2 and CO present the γ_i value immediately after target flash was found to be very nearly that for the clean metal as determined with no adsorbable gas admitted, whereas with H_2 present a much lower value, nearer that for a covered surface, was obtained (Fig. 6). We note that the first reading of γ_i is made in a time after the target is cooled which is about 5 to 10% of the time for a monolayer to form on the surface. From Fig. 6 we should perhaps conclude that the coverage immediately upon cooling is of the order of 75% of a monolayer.

The experimental facts concerning the anomalous behavior in hydrogen are these:

1. γ_i immediately after flash in H_2 is not that for clean W but about 80% of this value.
2. The tungsten surface appears to be covered immediately upon cooling with about 75% of a monolayer.
3. The low γ_i effect persisted after H_2 was removed from the apparatus for a period despite repeated target flashing in the best vacuum attainable and with CO present.
4. The low γ_i effect showed no tendency to diminish in amount or to disappear with repeated flashing in the presence of H_2.
5. The low γ_i effect did not appear to depend on length of target flash nor on whether the target was flashed once or several times before the γ_i measurement was made.
6. Not all the gas thought to be contained in the H_2 monolayer appeared as gaseous H_2 after a target flash to 2300°K (low Δp on flash).

One conclusion from the above experimental facts which seems inescapable is that the surface of the tungsten is covered with an appreciable fraction of a

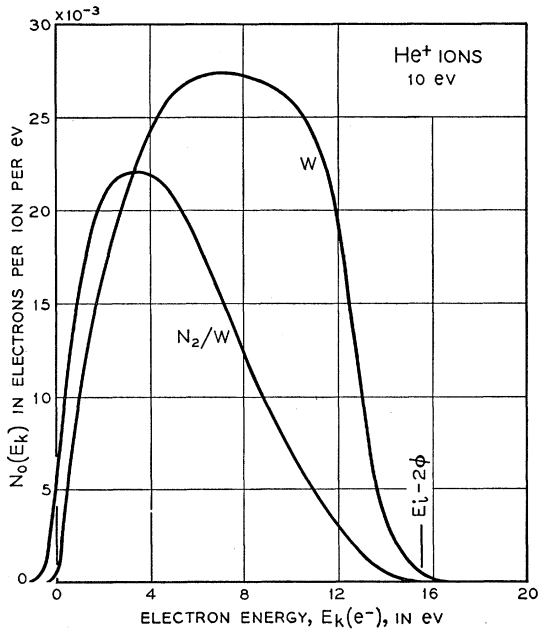

FIG. 12. Distributions in energy of electrons ejected by 10-ev He^+ ions from atomically clean tungsten (W) and tungsten covered with a monolayer of N_2 (N_2/W). Curve for N_2/W adjusted on V_{ST} (electron energy) scale according to 0.4-ev change in work function as N_2 monolayer forms (see text).

[8] J. C. P. Mignolet, Rec. trav. chim. 74, 685 (1955), reports an increase of 0.5 ev in the work function of tungsten on exposure to nitrogen.

monlayer essentially immediately upon cooling from the high temperature. The questions we should like to answer are: what is the gas which covers the surface and where does it come from?

It is possible to say that the gas cannot have been adsorbed out of the gas phase in the short time between cooling and γ_i measurement. We expect neither H_2 nor any product gas such as H_2O formed from dissociated H_2 and oxides on nearby surfaces to have an arrival rate at the target any greater than the gaseous H_2 present in the apparatus. In fact, to cover the target to 0.75 monolayer in the 30 seconds from cooling to first γ_i measurement would require an arrival rate twenty times that of the gaseous H_2 at the pressure used.

We also can perhaps rule out surface migration from the cool ends of the filament on the grounds that the temperature of the target as it cools remains for such a short time at temperatures below the lowest for an appreciable evaporation rate and above the lowest for an appreciable migration rate. This picture would require the steady migration of large quantities of gas on repeated flashes from the cool ends which have considerably smaller surface area than the target itself.

A possible explanation of this anomaly in H_2 is suggested by the behavior of tantalum with respect to residual gases.[9] It involves the absorption of about 75% of the hydrogen monolayer into the body of the metal when the temperature is suddenly raised. This would presumably occur as the temperature rises when the solubility has increased but before the evaporation rate from the surface has increased appreciably. After repeated flashing and cooling, the lattice could become saturated with hydrogen at room temperature. Thus on cooling the target, the gas absorbed from the monolayer on heating would have to reappear at the surface. This would account for the observed surface coverage on cooling.

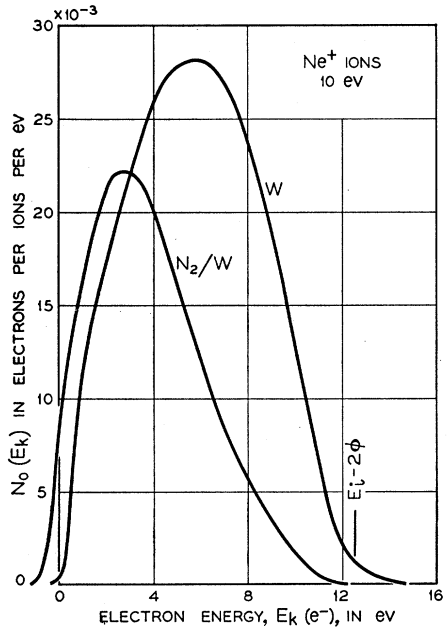

FIG. 13. Distributions in energy of electrons ejected by 10-ev Ne^+ ions from atomically clean tungsten (W) and tungsten covered with an N_2 monolayer (N_2/W). Energy scales adjusted for work function change caused by nitrogen monolayer.

[9] H. D. Hagstrum, Phys. Rev. **91**, 543 (1953).

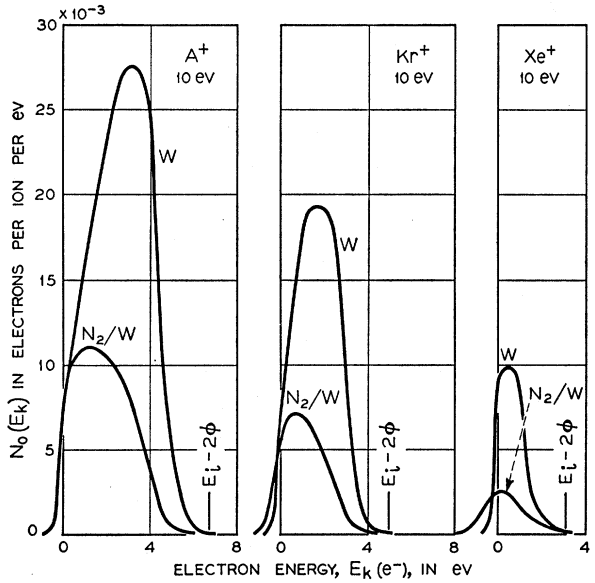

FIG. 14. Distributions in energy of electrons ejected by 10-ev A^+, Kr^+, and Xe^+ ions from clean tungsten (W) and tungsten covered with an N_2 monolayer (N_2/W). Energy scales adjusted for work function change caused by nitrogen monolayer.

Not sufficient experimentation was done at the time to warrant further discussion of the anomaly observed in H_2. Suffice it to say that the behavior was quite different from that in N_2 and CO, and is suggestive of a further use of the phenomenon of Auger ejection in the study of the reactions of gases with metal surfaces.

VII. DISCUSSION OF THE EFFECTS OF MONOLAYER ADSORPTION ON ELECTRON EJECTION BY IONS

We turn now to a discussion of the possible reasons for the changes in the characteristics of electron ejection from a metal by ions as the metal surface covers with a monolayer of foreign atoms. There are three results of monolayer adsorption which could have an effect on the electron ejection process. These are: (1) change in work function, φ; (2) changes in the variation of atomic energy levels near the metal surface; and (3) the greater probability of electron ejection by non-Auger processes.

It is perhaps fair to say that the change in work function of tungsten when a layer of N_2 adsorbs upon it has not been definitely established. However, in this discussion we shall investigate the effect of a change of 0.5 ev in φ.[8] The effects on the Auger ejection process of a simple increase of work function of 0.5 ev are the following. It is clear from Fig. 15 that the forms of the distributions in kinetic energy, N_i, of internally excited

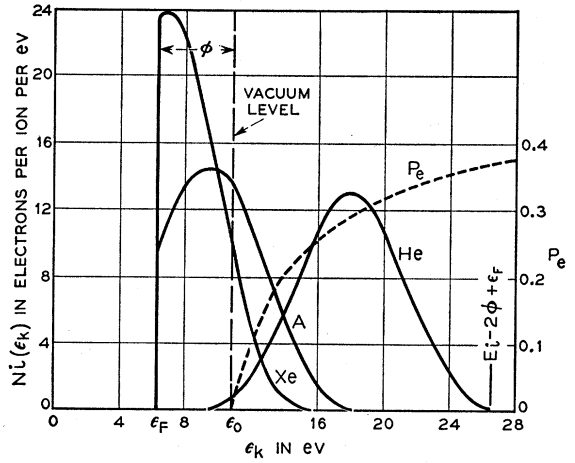

FIG. 15. Distributions in energy inside the metal of electrons excited in the Auger neutralization of He^+, A^+, and Xe^+ ions at a clean tungsten surface. The energy ϵ_k is measured above the bottom of the conduction band. The top of the conduction band is at ϵ_F and the vacuum level at ϵ_0. The probability of escape of these electrons from the metal is the curve P_e. All the curves of this figure are obtained from the theory discussed in reference 4 and are shown here as an aid in assessing the effect on Auger ejection of a change in work function φ.

electrons do not change if φ changes. They move in position by $-\Delta\varphi$ relative to the conduction band since their maximum energy on the ϵ_k scale lies approximately at $E_i-\varphi+\epsilon_F$. However, the vacuum level moves up in energy by $+\Delta\varphi$ relative to the conduction band and thus the P_e curve by $+2\Delta\varphi$ relative to the N_i function. All of this conspires to reduce the total yields, the areas under the N_0 curves in Fig. 16. It does not change appreciably the form of the N_0 distribution for an ion like He^+ where the N_i distribution lies almost entirely at energies above the vacuum level.

Values of γ_i computed for the clean and covered surface from Fig. 16 are compared with the measured values in Table IV. Here it is seen that a simple change in φ of 0.5 ev should result in γ_i changes which are considerably smaller than are observed. Furthermore it cannot account for the observed changes in form of the $N_0(E_k)$ function.

A change in the way atomic energy levels vary near the metal surface is a possible result of monolayer adsorption which will certainly affect the nature of the Auger ejection process. In the previously published theory,[4] account was taken of atomic energy level shifts near the metal surface. These are the results of image force attraction for the ion, Van der Waal's attraction, and repulsion by virtue of the exclusion principle at close approach. The effect of these variations is best seen perhaps on a potential energy diagram of the type developed in the theory.[4] In Fig. 17 such a plot is shown for the process of Auger neutralization of A^+. The potential curve 1 gives the variation of the initial

TABLE IV. Comparison of measured and computed γ_i values for clean and covered tungsten.

		He	Ne	A	Kr	Xe
Measured[a]	clean	0.290	0.210	0.095	0.050	0.013
	covered	0.180	0.130	0.045	0.017	0.002
Computed[b]	clean	0.279	···	0.050	···	0.012
	covered	0.250	···	0.030	···	0.004

[a] These are values measured for 10-ev ions; the covered values are for a monlayer of N_2. Data are taken from Figs. 8 and 9.

[b] The clean values are the same as those computed in reference 4 in which see Table XII and Fig. 28. The covered values correspond to a supposed increase in work function of 0.5 ev. These computed γ_i values are the areas under the theoretical $N_0(E_k)$ distributions of Fig. 16. Thus in this calculation the only effect of surface coverage is taken to be an increase in work function of 0.5 ev.

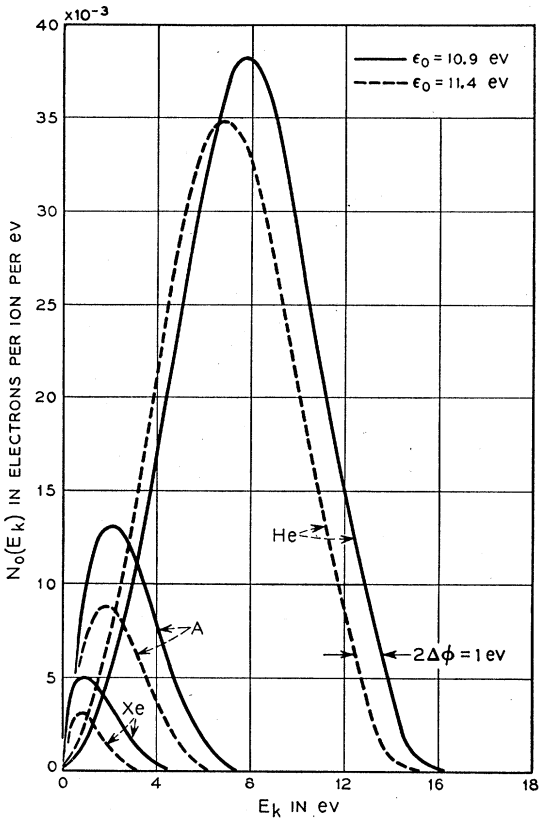

FIG. 16. Distributions in energy of electrons which leave the metal after having been excited in the Auger neutralization process. The full curves are for clean tungsten ($\varphi=4.5$ ev, $\epsilon_0=10.9$ ev) and are obtained from the N_i curves of Fig. 15. The dashed curves are for the metal with a 0.5-ev increase in work function ($\varphi=5.0$ ev, $\epsilon_0=11.4$ ev). E_k is the kinetic energy of the electrons outside the metal. γ_i values computed as the areas under these curves are listed in Table IV.

state of the process: $A^+ + ne_W^-$, the argon ion with n electrons in the tungsten. The final states of the process lie in the band between curves 2 and 3 depending on from where in the conduction band the two electrons involved in the process are removed. The final state is $A + e^- + (n-2)e_W^-$, the neutralized argon atom, a free electron, and $(n-2)$ electrons remaining in the tungsten. The Auger neutralization process corresponds in Fig. 17 to a vertical transition from curve 1 to one of the curves lying between curves 1 and 3. The length of the

vertical transition from curve 1 to the final curve between it and curve 3 gives the kinetic energy of the ejected electron. Let us assume that the transitions occur when the distance of the atomic particle from the metal surface lies in the stippled region of Fig. 17. All vertical transitions then must lie in this region.

We now ask what effect on a diagram like Fig. 17 we should expect the adsorption of a monolayer to have. In the first place, a small change in work function would shift curves 2 and 3 slightly with respect to curve 1, but this effect has already been discussed and will not be carried along further here. A possible change in form of the potential curves is arrived at as follows. We assume that the image force and Van der Waal's attractions as well as the region of high transition probability for the Auger process are unaffected by the interposition of a monolayer of a gas like nitrogen between the metal lattice and the incoming atomic particle. But we assume that the presence of this monolayer causes the repulsive forces arising from the exclusion principle to become effective at distances about one atom diameter farther from the metal surface than in the absence of the layer. This is indicated by the dashed lines in Fig. 17. It is now clear that for transitions which occur inside the stippled region of Fig. 17 there will result fewer faster electrons. Thus in a very qualitative fashion one can account for the reduction in γ_i and the change in form observed for the energy distribution functions.

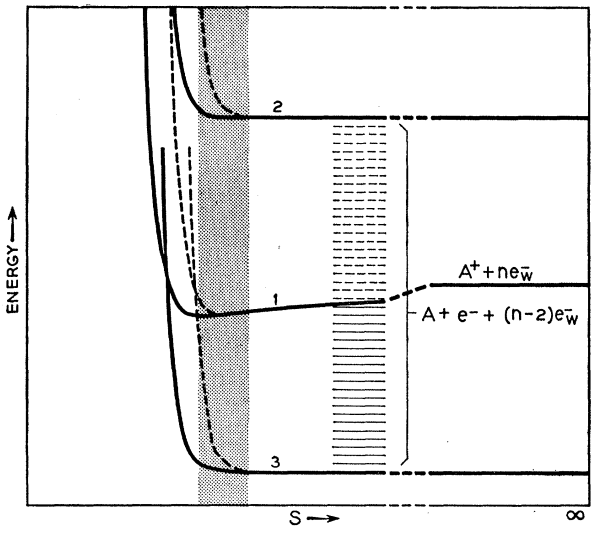

FIG. 17. Curves indicating the possible variations of atomic energy levels near a metal surface when the surface is clean and covered with a monolayer of gas. The full curves are for the clean surface, the dashed curves for the covered surface indicating repulsion of the incident particle at greater distances from the metal. Curve 1 gives the energy of the initial state as a function of distance of the atomic particle from the metal for the process of Auger neutralization of A^+ at a W surface. The final states lie between curves 2 and 3 and those energetically attainable lie below curve 1. This diagram is an extension of Fig. 20 of reference 4. The stippled region is that in which the Auger process most probably occurs.

The picture just presented most likely has some merit for very slow ions of all the noble gases and for the heavier ions at all energies used in the experiment. It cannot be the whole story, however, because it does not account for the observed variation with ion energy of the yield from a covered surface by the lighter noble gas ions. The theory of Auger neutralization by He^+ ions using potential curves like the dashed lines in Fig. 17 would still predict a reduction of γ_i with increase in ion energy. As seen in Fig. 10 the exact opposite is observed. To this author's mind, this can only mean that the process operative is not purely the Auger process but that there must also be electron ejection in a non-Auger process. We recall that even for the atomically clean surface there is strong evidence of such non-Auger processes setting in at energies above 400 ev with He^+.[1,2] It is not unreasonable then to suppose that such processes may begin at lower energies when a monolayer is present on the surface. Such processes are needed to explain the situation for the lighter ions which are those of highest velocity at a given energy. The nature of the non-Auger or kinetic ejection process is obscure but is most probably a release of bound electrons from surface atoms by impact of the ion. We note that the observed variation of γ_i with ion energy and the form of the $N_0(E_k)$distribution for the electrons ejected by non-Auger processes for He^+ of energy greater than 400 ev are like those observed here for the lighter ions incident on a surface covered with a monolayer.

The author wishes to acknowledge with thanks the help of several people. F. J. Koch and C. D'Amico recorded all the data presented here. The apparatus used was constructed by V. J. DeLucca, E. Deery, and A. A. Machalett. Several helpful discussions were had with J. A. Becker. D. J. Rose read the manuscript critically.